ARMY RESEARCH LABORATORY

Transparent Composite Utilizing Nonlinear Optical Polymers

by Daniel J. O'Brien, Joshua A. Orlicki, J. Derek Demaree, and James K. Hirvonen

ARL-TR-4287   **September 2007**

NOTICES

Disclaimers

The findings in this report are not to be construed as an official Department of the Army position unless so designated by other authorized documents.

Citation of manufacturer's or trade names does not constitute an official endorsement or approval of the use thereof.

Destroy this report when it is no longer needed. Do not return it to the originator.

Army Research Laboratory

Aberdeen Proving Ground, MD 21005-5069

Transparent Composite Utilizing Nonlinear Optical Polymers

**Daniel J. O'Brien, Joshua A. Orlicki, J. Derek Demaree,
and James K. Hirvonen**
Weapons and Materials Research Directorate, ARL

REPORT DOCUMENTATION PAGE

1. REPORT DATE *(DD-MM-YYYY)*	2. REPORT TYPE	3. DATES COVERED (From - To)
September 2007	Final	October 2004–September 2005

4. TITLE AND SUBTITLE	5a. CONTRACT NUMBER
Transparent Composite Utilizing Nonlinear Optical Polymers	
	5b. GRANT NUMBER
	5c. PROGRAM ELEMENT NUMBER

6. AUTHOR(S)	5d. PROJECT NUMBER
Daniel J. O'Brien, Joshua A. Orlicki, J. Derek Demaree, and James K. Hirvonen	622105.AH84
	5e. TASK NUMBER
	5f. WORK UNIT NUMBER

7. PERFORMING ORGANIZATION NAME(S) AND ADDRESS(ES)	8. PERFORMING ORGANIZATION REPORT NUMBER
U.S. Army Research Laboratory ATTN: AMSRD-ARL-WM-MA Aberdeen Proving Ground, MD 21005-5069	ARL-TR-4287

9. SPONSORING/MONITORING AGENCY NAME(S) AND ADDRESS(ES)	10. SPONSOR/MONITOR'S ACRONYM(S)
	11. SPONSOR/MONITOR'S REPORT NUMBER(S)

12. DISTRIBUTION/AVAILABILITY STATEMENT

Approved for public release; distribution is unlimited.

13. SUPPLEMENTARY NOTES

14. ABSTRACT

Polymer composites are attractive candidates for lightweight armor applications and can be made transparent by matching constituent refractive indices (RIs). Unfortunately, RI matching is difficult since the indices must be matched to approximately the third decimal place, and the matrix RI is very sensitive to factors such as temperature and stress state. Therefore, index-matched systems are transparent only over a narrow temperature range. In order to capitalize on the superior properties of polymer composites in transparent armor applications, novel techniques are needed that can dynamically account for small changes in the RI. In this report, we investigate transparent composites that utilize polymer matrices whose RIs can be modulated in real time. Glass-reinforced composites are manufactured using polymers that incorporate nonlinear optical (NLO) chromophores—small molecules whose RI can be changed with an applied electric field. We find that by utilizing typical NLO chromophores, the polymer matrix has insufficient electro-optical response for significant RI modulation.

15. SUBJECT TERMS

composite, transparent, electro-optical, refractive index, epoxy, nonlinear optical

16. SECURITY CLASSIFICATION OF:			17. LIMITATION OF ABSTRACT	18. NUMBER OF PAGES	19a. NAME OF RESPONSIBLE PERSON Daniel O'Brien
a. REPORT UNCLASSIFIED	b. ABSTRACT UNCLASSIFIED	c. THIS PAGE UNCLASSIFIED	UL	30	19b. TELEPHONE NUMBER (*Include area code*) 410-306-0843

Contents

List of Figures

List of Tables

INTENTIONALLY LEFT BLANK.

1. Introduction

In the effort to field a more agile and survivable fighting force, there is an increasing need in the U.S. Army for lightweight, transparent armor materials. Polymer composites are attractive candidates for lightweight armor applications and can be made transparent by matching constituent refractions indices (RIs). Unfortunately, RI matching is difficult since the indices must be matched to approximately the third decimal place, and transparency becomes increasingly sensitive to index variations as volume fraction increases. For example, Iba and Kagawa (*1*) showed that for $v_f = 0.10$, the transmittance decreases by 20% for a fiber-matrix index mismatch of only 0.0005.

The problem is further complicated by the stress and temperature dependence of the RI. Because of processing-induced residual stresses, a given glass and polymer system may individually have identical indices but become index mismatched after fabrication into a composite. Furthermore, in fiber-reinforced systems, the index of the polymer matrix changes much faster with temperature than that of the fiber, and in rubber-toughened polymers, the index of the rubber phase changes much faster than that of the matrix. Therefore, as figure 1 shows, these index-matched systems are transparent only over a narrow temperature range (*2*).
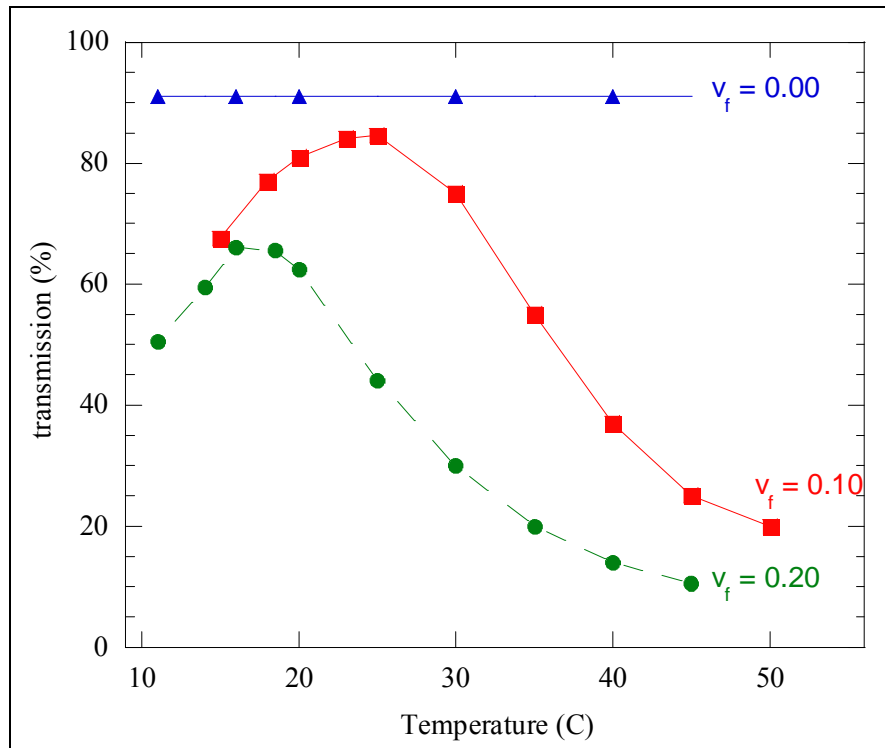

Figure 1. Temperature-dependent transmission of optical glass/PMMA composite
for various fiber volume fractions (*2*).

1

In order to capitalize on the superior properties of polymer composites in transparent armor applications, novel techniques are needed that can dynamically account for small changes in the RI. The goal of this research is to manufacture transparent composites using polymer matrices whose RIs can be controlled with an applied electric field. In this work, the polymer is rendered electro-optically active through the incorporation of a nonlinear optical (NLO) chromophore or dye.

NLO polymers undergo a change in RI in response to an applied electric field with

$$\Delta n = -\frac{1}{2} n^3 r E , \qquad (1)$$

where n is the index of refraction, r is the electro-optic coefficient, and E is the electric field strength (*3*). Usually, polymers such as urethanes, polyesters, epoxies, or acrylics are rendered electro-optically active through the addition of a chromophore that is mixed with the polymer, is incorporated into the polymer backbone, or is grafted as a side chain. Electro-optic coefficients of NLO polymers are typically $20-30\times10^{-12}\ ^m\!/_V$ and can be as high as $100\times10^{-12}\ ^m\!/_V$.

NLO polymers have received much interest recently. A wide variety of polymers have been rendered electro-optically active through the incorporation of chromophores. Ambrosanio et al. (*4*) incorporated a chromophore derived from 4[N,N-bis(2-hydoxyethyl)amino]-benzaldehyde into a polyester network. Thackara et al. (*5*) incorporated the chromophore nitroamino tolane as a side chain to polymethlmethacrylate (PMMA). Mao et al. (*6*) studied the concentration dependence on optical properties of a trifunctional disperse red-type chromophore in urethane networks. However, with the overwhelming interest in using NLO polymers for low-cost optoelectronic device fabrication, NLO polymers have not yet been incorporated into structural composites.

The polymers studied so far cover a wide range in RI (~1.45–1.65). However, it is difficult to find a polymer that is both easy to process into a composite and sufficiently matches the RI of E-glass or S2 glass. We chose E-glass as the reinforcement, and we chose an epoxy system that allows for manipulation of the neat resin's RI through the variation of constituent concentration.

In this work we attempted to provide a proof-of-concept demonstration of an electro-optically active composite. This is accomplished by manufacturing a RI-matched E-glass/NLO epoxy composite. The composite is tested for electro-optical activity by measuring the transmission intensity through the specimen with and without an applied electric field. Presumably, if the composite is indeed electro-optically active, an applied electric field would result in a decrease in transmitted intensity as the composite matrix switches from matched to unmatched. Of course, in a fielded application of this technology, the system would likely be designed to maximize transmission. Here, we are simply interested in observing a change in transmission. In addition to demonstrating this proof of concept, we also explore the synthesis of new, high-response chromophore molecules.

In the sections that follow, the design of an electro-optically active composite is discussed first, along with guidelines for synthesizing high-response dye molecules. Section 3 of this report presents the measurement of the matrix RI. These RI measurements enable the proper choice of matrix in the design of the NLO composite. Procedures for construction and testing of the NLO composites are presented next, followed by methods for synthesizing high-response chromophore. The report concludes with results and discussion.

2. Approach

2.1   NLO Composite Design

The envisioned transparent material (figure 2a) will consist of the NLO composite sandwiched between transparent electrodes such as indium tin oxide. Assuming a typical electro-optic coefficient of $25 \times 10^{-12}\ ^m\!/_V$ and a composite thickness of 100 μm, the index of refraction could be varied by 0.005 with a 10-kV potential. While a change of 0.005 may seem small, it will provide significant flexibility in compensating for matrix index variations. For example, considering a polymer with a typical thermo-optic coefficient of ~0.0001 ºC^{-1}, a change in index of 0.005 corresponds to a 50 ºC extension of the transparency window of an index-matched composite. This technique will also allow for the compensation of much smaller variations in index, such as those due to residual stresses.
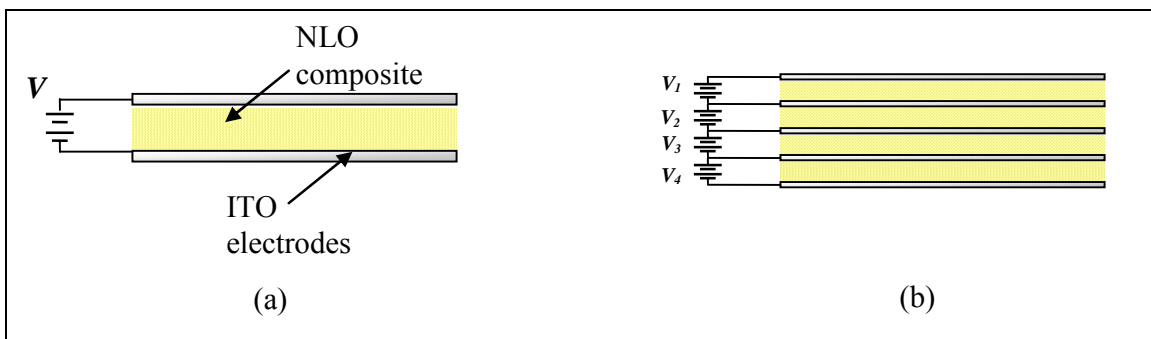
Figure 2. Transparent NLO composite: (a) individual NLO composite layer and (b) multilayer stack.

Individual NLO composites can then be stacked up to construct a material of arbitrary thickness (figure 2b). Such a structure will permit the variation of the electric field through the thickness of the composite to compensate for temperature and stress gradients.

Using specimens like those in figure 2a, we focused on the demonstration of transparency control through the manipulation of matrix RI. In this effort, we used a common NLO chromophore or dye, disperse red 1 (DR1), incorporated into an epoxy matrix reinforced with E-glass spheres.

2.2   Chromophore Synthesis

Parallel to the effort to demonstrate transparency control in a polymer composite using a common, commercially available dye, we also pursued synthesis of high-response dyes. A wide array of these dyes, composed of high-aspect ratio-conjugated systems, have been reported in the literature. They generally consist of push-pull-type electron-donating and electron-withdrawing groups, resulting in highly polarizable molecules. The synthesis of these dyes is well known, though, generally several synthetic steps and chromatographic purification are required to prepare them.

This work sought to develop novel high-aspect ratio-conjugated molecules with both electron-donating and electron-withdrawing poles. The materials envisioned should be accessible in three synthetic steps, with minimal chromatography required for purification. The chemistry selected for this synthetic effort has been heavily promoted by Kolb et al. (*7*) as a "click" chemistry or "spring-loaded" reaction. In the literature, this terminology is used to refer to high-fidelity reactions that yield thermodynamically favored products. The most efficient click reaction to date is Huisgen's 1,3-dipolar cycloaddition of an azide and an alkyne, yielding a 1,4-disubstituted triazole (figure 3). This conjugated linkage is thermally stable and is formed rapidly in the presence of copper(I) catalyst, which is generally formed in situ from copper(II) sources and a reducing agent such as ascorbic acid.
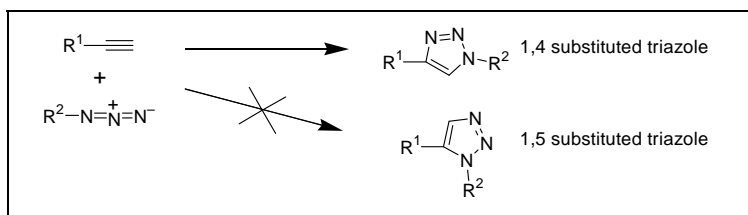
Figure 3. Cu(I)-catalyzed 1,3 dipolar cycloaddition products.

To test the facility of the click chemistry approach, a pair of azides (1, 2) was generated from commercially available alkyl halides to perform model reactions. They are shown in figure 4, along with their reaction with the phenylacetylene to generate the desired triazole products (3, 4). The copper(I)-catalyzed cycloaddition may also take place with a cyanate group instead of an acetylene, albeit at a reduced rate. This avenue was explored with a nitrosubstituted phenyl-cynate, as electron withdrawing groups are reported to accelerate the cycloaddition. However, the reaction remained sluggish, and undesired side products were predominantly obtained. Therefore, the effort to develop tetrazoles using this reaction pathway was abandoned. A model compound was also procured to test the enolization of a keto-aromatic system. Deoxybenzoin was used to prepare compound 5 as a mimic for the α-triazole ketone prepared for this project.

4
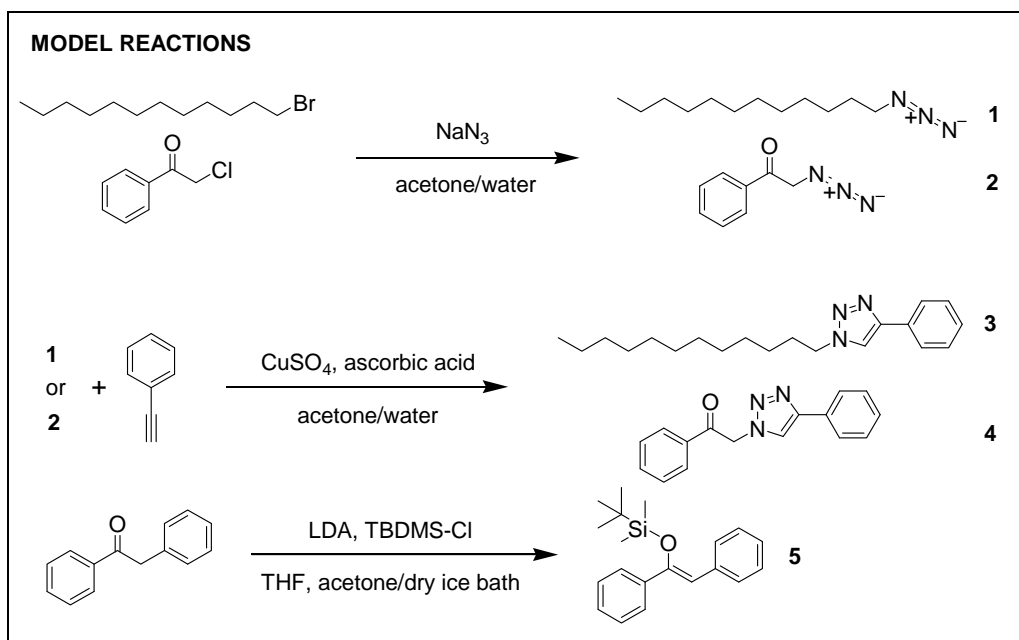
Figure 4. Model click reactions and enolization.

The specific synthetic scheme pursued for an NLO material is outlined in figure 5. An α-keto halide was to undergo substitution with sodium azide (6), followed by cyclization with phenylacetylene to yield a conjugated triazole system (7). In order to generate a fully conjugated system, though, the α-keto triazole had to be transformed to the enol form. Several attempts were made to generate the enol form and then trap it as either the methyl or silyl ether. Unfortunately, excessive side products were obtained from all attempts, so an alternative route may need to be investigated.
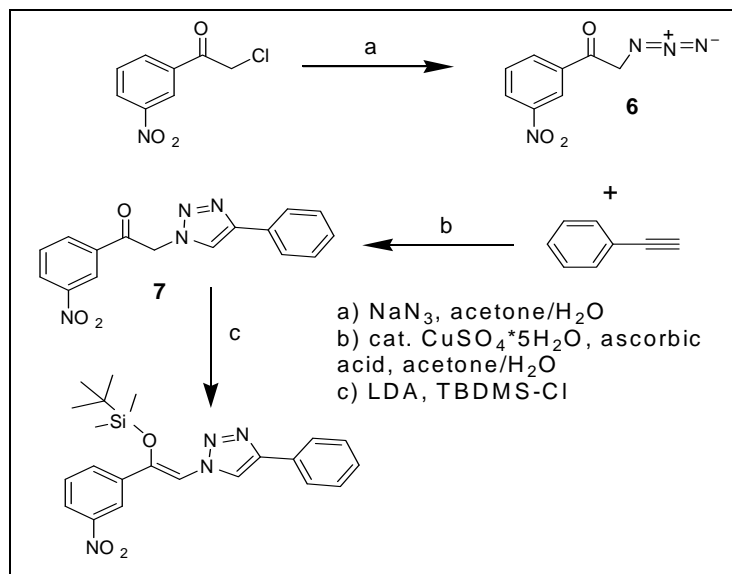
Figure 5. Preparation of fully conjugated NLO candidates.

3. Experimental Procedure

3.1 RI Measurements

3.1.1 Neat Resin

Composite specimens were manufactured using a common glass reinforcement (E-glass) in the form of 35-μm glass beads (Spheriglass 3000E, Potters Industries, Valley Forge, PA) with an RI of 1.55. Since we do not expect control over the matrix RI much beyond ±0.001, it is important to match the RIs of matrix and reinforcement as close as possible to allow for maximum transparency. This task is complicated by the fact that inclusion of the NLO chromophore in the matrix will tend to increase the RI.

Unfortunately, RI data are limited for all but a few polymers. For epoxy (the matrix chosen for this work), the RI is a function of the epoxy prepolymer as well as the curing agent. We measured the RI of various epoxy prepolymers cured with various curing agents. Table 1 shows the different epoxy systems studied.

Table 1. List of epoxide/curing agent systems tested for RI.

| Epoxy	Curing Agent
Epon 828 (bisphenol A epoxide)	Triethylenetriamine (TETA)
Epon 828 (bisphenol A epoxide)	EPIKURE 3300
Epon 828 (bisphenol A epoxide)	Amicure PACM
Epon 862 (bisphenol F epoxide)	EPIKURE 3300
DER 332 (bisphenol A epoxide)	EPIKURE 3300
Eponex 1510	TETA
Eponex 1510	Amicure PACM
Epotek 301-2	Unknown amine
Spurr epoxy	Unknown anhydride

After measuring the RI of the epoxies listed in table 1, we chose two that had significantly different RIs (Epon 828/TETA and Eponex 1510/TETA) and measured the RI of various mixtures of these two systems.

The RI measurements were performed using and Abbé refractometer (model DRM2, Atago Co. Ltd., Tokyo, Japan) at wavelengths of 589, 750, and 1100 nm. Prismatic epoxy specimens were cured in open-face silicone rubber molds approximately $50 \times 10 \times 10$ mm. Glass slides treated with a silicone mold release were placed over the open face of the mold to provide a smooth surface with which to make the RI measurement.

In addition to the cured epoxy samples, we also measured the RI of uncured 828/1510 mixtures over a range of mix ratios.

3.1.2 Doped Resin

To determine the effect of the NLO chromophore on the matrix RI, several films were manufactured with various amounts of DR1 (Sigma-Aldrich, St. Louis, MO), the NLO chromophore dye used in this study. These specimens were manufactured by dissolving 5% DR1 in tetrahyrdofuran (THF). Then, the dye solution was added to an epoxy resin mixture of equal parts 1510 and 828. The THF/dye/epoxy resin mixture was then placed in the oven overnight at 65 ºC to drive off the THF. Next, a stoichiometric amount of TETA was added to the mixture, and a few drops were placed on a silicone-treated glass slide. A second silicone-treated slide was placed on top, and three glass coverslips were placed between the slides to control film thickness. Finally, the slides were clamped together with binder clips and allowed to cure for 1 hr at 93 ºC. After curing, the films were cut into ~40- $\times$ 6-mm-strips, and the RI was measured at 750 nm.

3.2 NLO Specimen Manufacture

Using the RI measurements as our guide, we chose to manufacture epoxy/E glass/DR1 composites using an 86/14% mixture of 1510/828 resins cured with a stoichiometric amount of curing agent. This ratio was chosen so that at 10% DR1, the RI of the matrix closely matches that of the E-glass spheres at 1000 nm.

The matrix was prepared in a manner similar to that just described except that 20% (by weight) glass spheres were added to the mixture. A few drops of the uncured composite were placed between glass slides, and Teflon film (70-µm thick) was placed between the slides at either end to act spacers. The slides in these experiments were coated with a thin, transparent layer of conductive indium tin oxide (ITO) on one side. As figure 6 shows, the slides were oriented so that the ITO-coated sides faced one another, and a small portion extended from each end to provide electrical access. The specimens were cured for 1 hr at 93 ºC. A power supply (2410 Sourcemeter, Keithly Inc., Cleveland, OH) was used to apply a 1-kV electric potential applied across the leads. This poling voltage serves to align the polar chromophore molecules rendering the specimen noncentrosymmetric, a criterion for nonlinear optical behavior. Two specimens were made with chromophores. One was cured under the electric field, and one was left unpoled. Also, as a control, one specimen was manufactured without dye.

To determine if increased chromophore mobility would lead to higher electro-optic activity, we manufactured specimens as just described, but without curing agent. In these specimens, only 2.5% DR1 was used because the dye tended to precipitate out of solution at higher concentrations.
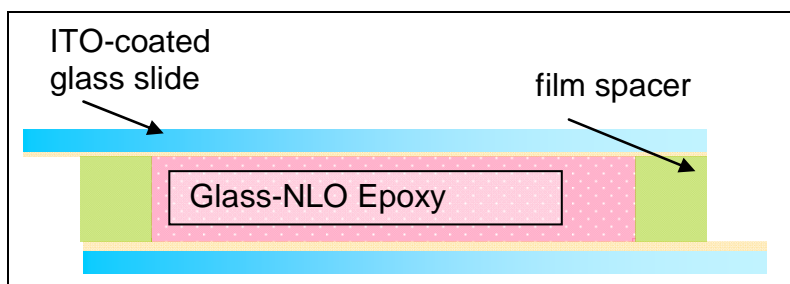
Figure 6. Schematic of electro-optically active composite specimen.

3.3   Deposition of Transparent Electrodes

To deposit electrically conductive and optically transparent ITO coatings, one must either deposit onto a heated substrate (not suitable for polymers) or bombard the growing surface with energetic ions. ITO coatings were deposited via ion beam-assisted deposition by evaporating (90 In/10 Sn) ITO at 0.1 nm/s in the presence of an oxygen ion beam (100–300 eV; 50–100 $\mu A/cm^2$). A critical thickness of 50–100 nm was needed to produce a continuous layer on glass or polymeric substrates.

3.4   Optical Transmission Experiments

The optical transmissions of the NLO specimens were tested under various electrical fields using a UV-Vis spectrometer (Model Cary 5G, Walnut Creek, CA). The experiment, shown schematically in figure 7, was performed immediately after curing the specimen and cooling to room temperature.
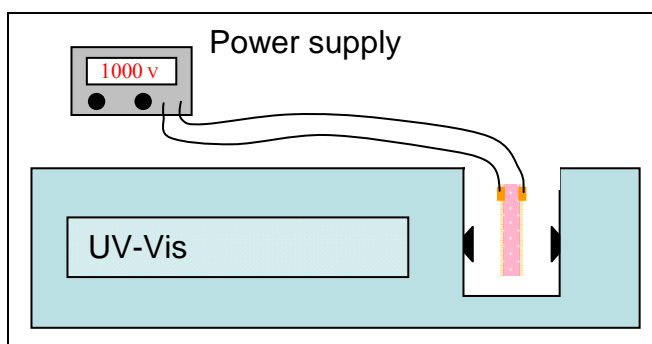
Figure 7. Schematic of experiment to test for electro-optic activity.

3.5   Chromophore Synthesis

3.5.1 Azide Installation – Alkyl (Compound 1)

Dedecyl bromide (2.49 g, 10 mmol) was charged to a 100-mL round bottom flask (RBF). Then, ~35 mL of 4:1 acetone:H_2O was added to the flask. The aliphatic chain exhibited limited solubility in this matrix, but rapid agitation (stirring with magnetic stir bar) resulted in a homogenized suspension. Then, sodium azide was added (1.30 g, 20 mmol, 2 equivalents), and

the RBF was placed in an oil bath. The temperature was adjusted so the solution refluxed, and a condensation column was added to the flask to maintain the organic solvent in the reaction system. The reaction was monitored periodically using thin layer chromatography (TLC) on silica plates, eluted with hexanes, developed with $KMnO_4$ solution. After ~20 hr, the reaction was nearly complete and very little residual starting material was detected. The condensation column was removed from the flask, and the majority of the acetone was allowed to evaporate. After being reduced to ~1/4 of the initial volume, the remaining solution was poured into 120 mL of H_2O, from which was then extracted 2- $\times$ 120-mL hexanes. The combined organics were then washed with 1- $\times$ 120-mL brine, dried with magnesium sulfate, filtered, and the organics were removed by rotary evaporation. The resulting oil was clear with a slight yellow cast. It was dried for 16 hr in a vacuum oven (50 °C, 25-in Hg vacuum). ^{1}H NMR (600 MHz, $CDCl_3$, δ): 3.25 (t, J = 7 Hz, 2 H); 1.59 (quint, J = 7.2 Hz, 2 H); 1.36 (mult, 2 H); 1.26 (s, 16 H); 0.88 (t, J = 7.1 Hz, 3 H). ^{13}C NMR (150 MHz, $CDCl_3$, δ): 51.46, 31.89, 29.6, 29.52, 29.46, 29.31, 29.13, 28.82, 26.7.

3.5.2 Click Reaction – Phenylethynylene and Alkyl Azide (Compound 3)

A magnetic stir bar along with phenyl acetylene (0.204 g, 2 mmol) was charged to a 20-mL scintillation vial. Then, ~4-mL acetone was added, along with ~1-mL water. An aqueous solution of ascorbic acid was added (~0.775 mL, 0.2 mmol), along with dodecyl azide (0.416 g, 2 mmol). Then the copper sulfate solution was added (0.5 mL, 0.1 mmol) to generate the Cu(I) salt to catalyze the Huisgen 1,3 dipolar cycloaddition (i.e., the click chemistry). The vial was placed on a hot plate at the lowest heat setting, and the contents were stirred. After ~1.5 hr, the vial was removed. Crystals had formed in the solution. An additional 10 mL of H_2O was added to the cooled solution, and the crystals were filtered on a fritted glass filter (coarse). The crystals were dried for 36 hr in a vacuum oven (50 °C) and resulted in a fibrous, canary yellow solid (0.560 g, 88.6% yield). ^{1}H NMR (600 MHz, $CDCl_3$, δ): 7.83 (d, J = 7.9 Hz, 2 H); 7.74 (s, 1 H); 7.41 (t, J = 7.5 Hz, 2 H); 7.32 (J = 7.5 Hz, 1 H); 4.37 (t, J = 7.4 Hz, 2 H); 1.93 (mult, 2 H); 1.34 (br-s, 2 H); 1.33 (br-s, 2 H); 1.25 (br-s, 14 H); 0.88 (t, J = 9 = 7 Hz, 3 H). ^{13}C NMR (150 MHz, $CDCl_3$, δ): 147.7, 130.8, 128.8, 128.1, 125.7, 119.4, 50.4, 31.9, 30.4, 29.6, 29.5, 29.4, 29, 26.5, 22.7, 14.1.

3.5.3 Azide Installation – α-Azide (Compound 2)

Two-chloro acetophenone (1.55 g, 10 mmol) was charged to a 100-mL RBF. Acetone (~25 mL) was then added to the flask. After the acetophenone had dissolved, ~8 mL of H_2O was added and a homogeneous solution resulted. Then sodium azide was added (1.3 g, 20 mmol, 2 equivalents), and the RBF was placed in an oil bath. The temperature was adjusted so the solution refluxed, and a condensation column was added to the flask to maintain the organic solvent in the reaction system. The reaction was monitored periodically using TLC on silica plates, eluted with 5:1 hexanes:EtOAc, and visualized with 254 nm of light. After ~4 hr, the reaction was complete and no residual starting material was detected. It is important to stop the

reaction soon after the consumption of the starting material, as additional side products are generated after the azide is formed. The condensation column was removed from the flask and the majority of the acetone was allowed to evaporate. After being reduced to ~1/4 of the initial volume, the remaining solution was poured into 120 mL of H_2O, from which was then extracted 2- × 120-mL CH_2Cl_2. The combined organics were then washed with 1- × 120-mL brine, dried with magnesium sulfate, filtered, and the organics were removed by rotary evaporation. The resulting crude material was a dark red oil. This was purified by passing it through a plug of silica gel, eluting with 40% CH_2Cl_2 in hexanes. The resulting oil was yellow. It was dried for 16 hr in a vacuum oven (25 °C, 25-in Hg vacuum). ^1H NMR (600 MHz, $CDCl_3$, δ): 7.89 (d, J = 7.4 Hz, 2 H); 7.61
(t, J = 7.3 Hz, 1 H); 7.49 (t, J = 7.5 Hz, 2 H); 4.55 (s, 2 H). ^{13}C NMR (150 MHz, $CDCl_3$, δ): 193.2, 134.4, 134.2, 129, 127.9, 54.9.

3.5.4 Click Reaction – Phenylethynylene and Azido-Acetophenone (Compound 4)

A magnetic stir bar along, with phenyl acetylene (0.323 g, 3.1 mmol), was charged to a 50-mL RBF. Then, ~7 mL acetone was added, along with ~2-mL water. An aqueous solution of ascorbic acid was added (~2.27 mL, 0.63 mmol), along with the azido-acetophenone (0.508 g, 3.1 mmol). Then, the copper sulfate solution was added (1.051 mL, 0.32 mmol) to generate the Cu(I) salt to catalyze the Huisgen 1,3 dipolar cycloaddition (i.e., the click chemistry). The RBF was placed in an oil bath at 65 °C. A precipitate formed almost immediately upon the addition of the $CuSO_4$. After ~2.25 hr, the flask was removed from the oil bath and allowed to cool. Consumption of the starting materials had been confirmed by TLC of the reaction mixture (9:1 hex:CH_2Cl_2). The precipitate was slurried in an additional 15 mL of H_2O, and was isolated by filtration. The solid was dried for 36 hr in a vacuum oven (50 °C) and resulted in a tan, powdery solid (0.752 g, 90.4 % yield). ^1H NMR (600 MHz, d_6-DMSO, δ): 8.3 (s, 1 H); 8.04 (d-d, J = 7.2 Hz, 1.2 Hz, 2 H); 7.82 (d-d, J = 8.3 Hz, 1.8 Hz, 2 H); 7.66 (t, J = 7.6, 1 H); 7.53 (t, J = 8.2, 2 H); 7.39 (t, J = 7.8 Hz, 2 H); 7.28 (t, J = 7.3 Hz, 1 H); 6.1 (s, 2 H). ^{13}C NMR (150 MHz, d_6-DMSO, δ): 191, 146.3, 133.7, 130.3, 128.4, 128.3, 127.7, 127.3, 124.8, 122.2, 55.4. (Note: only observed four methylene/quaternary ^{13}C, expected five, perhaps two overlay at 130.3 ppm, as intensity is greater than expected.)

3.5.5 Model Silyl Enol Ether Formation, Deoxybenzoin (Compound 5)

Di-isopropylamine (0.750g, 7.4 mmol) and dry THF (~4 mL) were charged to a 25-mL oven-dried flask with a stir bar. The flask was placed, with stirring, in a dry ice/acetone bath, and n-butyl lithium was added via syringe, dropwise (2.8 mL, 2.8 M, 1.05 equivalents) over 20 min. After the addition, the contents were allowed to stir in the bath until the dry ice was gone, and the solution was allowed to come to room temperature.

Deoxybenzoin (1.42 g, 7.2 mmol) and dry THF (15 mL) were charged to a 100-mL RBF equipped with a stir bar. The flask was lowered into an ice bath, and over a span of 20 min, the lithium diisopropylamide generated in the first flask was transferred by syringe. After ~40 min,

the flask was removed from the ice bath and was allowed to come to room temperature. After 1 hr at room temperature, TBDMS-Cl (1.110 g, 7.35 mmol) in dry THF (3 mL) was added to the flask (which was back in an ice bath) over 10 min. The contents of the flask were then allowed to come to room temperature and reacted for 16 hr.

The solvents were removed by rotary evaporation and yielded a precipitate and an oil. Examination by TLC indicated both starting material and product present. The oil and solid were dissolved in $CHCl_3$ and slurried with ~20-g silica gel. After removing the solvent, the silica gel was loaded onto a short plug of silica gel, which was eluted with hexanes. The desired product was isolated in 2- × 150-mL fractions of hexanes. Note: excess ^1H observed due to impurities. Comparison with starting material indicates new singlet at 6.16 ppm arising from ene-proton from trapped enol. ^1H NMR (600 MHz, $CDCl_3$, δ): 8.03 (mult, 1 H); 7.67 (d, J = 7, 2 H); 7.61 (d, J = 7, 2 H); 7.4–7.3 (br-multiplets, 6 H), 7.18 (mult, 1 H); 6.13 (br-s, 1 H), 1 (s, 9 H); 0.19 (s, 6 H). ^{13}C NMR (150 MHz, $CDCl_3$, δ): 151.1, 140.2, 136.6, 128.9, 128.1, 127.9, 126.3, 126, 125.7, 110.9, 25.9, 18.3, –3.9.

3.5.6 Azide Installation – α Azide With Nitro Group (Compound 6)

After 3-nitro-2'-chloroacetophenone (2.44 g, 10 mmol) was charged to a 100-mL RBF, acetone (~20 mL) was added to the flask. After the solid had dissolved, ~10 mL of H_2O was added, and the flask was placed in a warm oil bath (~50 °C) to maintain homogeneity of the solution. Then, sodium azide was added (1.3 g, 20 mmol, 2 equivalents). An immediate color change was observed: the solution turned orange where the sodium azide dissolved and spread to the rest of the flask upon mixing. After 5 min, the flask was pulled from the oil bath and N_2 was passed over the top of the flask to reduce the acetone concentration. A TLC performed at this stage revealed full reaction of the starting material (elution in 1:1 CH_2Cl_2:hexanes). The reduced-volume solution was poured into 100 mL of CH_2Cl_2, and extracted with 1 × 125 mL of H_2O. The organics were removed, and the water layer was washed with 1 × 125 mL of CH_2Cl_2. Then, the combined organics were washed with 1 × 125 mL of brine and dried over magnesium sulfate. After filtration, the CH_2Cl_2 was removed via rotovap to give a red oil, which precipitated/crystallized upon sitting. ^1H NMR (600 MHz, $CDCl_3$, δ): 8.72 (t, J = 2.2 Hz, 1 H); 8.48 (d-d-d, J = 8.4, 2.2, 1.2 Hz, 1 H); 8.26 (d-t, J = 8.4, 1.3 Hz, 1 H); 7.75 (t, J = 7.9 Hz, 1 H); 4.63 (s). ^{13}C NMR (150 MHz, $CDCl_3$, δ): not recorded.

3.5.7 Click Reaction – Phenylethynylene and Nitro-Azido-Acetophenone (Compound 7)

A magnetic stir bar, along with the nitro-azido-acetophenone (0.940 g, 4.56 mmol), was charged to a 100-mL RBF. Then, ~20 mL of acetone was added, followed by the phenyl acetylene (0.471 g, 4.61 mmol, 1.01 eq). An aqueous solution of ascorbic acid (1.76 mL, 0.519 M, 0.913 mmol) and copper sulfate (1.59 mL, 0.287 M, 0.456 mmol) were combined to generate the Cu(I) solution, which was then added to the acetone solution. The flask was placed in an oil bath at ~115 °C. The contents of the flask quickly began to boil and a precipitate appeared. The flask was removed from the heat after ~10 min, and TLC (100% CH_2Cl_2 eluent) determined that no

starting material remained. The precipitate was slurried in ~15 mL of H_2O and was isolated by filtration. The solid was dried for 16 hr in a vacuum oven (50 °C) and resulted in a tan, powdery solid (1.239 g, 88.1% yield). ^1H NMR (600 MHz, d_6-DMSO, δ):   8.79 (t, J = 1.8 Hz, 1 H); 8.56 (d-d, J = 8.3, 1.4 Hz, 1 H); 8.52 (s, 1 H); 8.51 (d, J = 10 Hz, 1 H); 7.93 (t, J = 8.1 Hz, 1 H); 7.89 (d-d, J = 8.1, 1.2 Hz, 2 H); 7.47 (t, J = 7.8 Hz, 3 H); 7.35 (t, J = 7.4 Hz, 2 H); 6.38 (s, 2 H). ^{13}C NMR (150 MHz, d_6-DMSO, δ): 191, 147.9, 146.2, 135.2, 124.2, 130.6, 130.5,128.8, 128.1, 127.7, 125, 122.8, 122.5, 56.1.

4. Results and Discussion

4.1 RI Measurements

Table 2 shows the results of the RI experiments of various epoxies. Of the materials tested, all of the bisphenol A and bisphenol F systems cured with an amine had RIs between 1.57 and 1.6. The anhydride-cured system had the lowest RI (1.49). However, the material had a brownish color and a very long cure time. The hydrogenated epoxy (Eponex 1510), when cured with the same amines as the bisphenol A system, had an RI of ~1.52.

Table 2. Measured RI of various epoxies.

Epoxy	Curing Agent	RI (589 nm)
Epon 828 (bisphenol A epoxide)	TETA	1.587
Epon 828 (bisphenol A epoxide)	EPIKURE 3300	1.575
Epon 828 (bisphenol A epoxide)	Amicure PACM	1.567
Epon 862 (bisphenol F epoxide)	EPIKURE 3300	1.573
DER 332 (bisphenol A epoxide)	EPIKURE 3300	1.599
Eponex 1510 (hydrogenated epoxide)	TETA	1.525
Eponex 1510 (hydrogenated epoxide)	Amicure PACM	1.521
Epotek 301-2 (bisphenol A epoxide)	Unknown amine	1.576
Spurr epoxy	Unknown anhydride	1.494

As previously mentioned, it is important in this work to match the RI of the epoxy and the glass reinforcement as closely as possible. Our approach was to search for two epoxies with RIs that bracket the RI of the E-glass (1.55) and to use a mixture of the two systems to choose the correct matrix RI. To test this approach, we measured the RI of mixtures of Eponex 1510 and Epon 828 cured with TETA. Choosing these two resins is convenient since they use the same curing agents, have similar reaction rates, and are likely to have similar reaction mechanisms.

Figure 8 shows the RI of TETA-cured 828/1510 mixtures at three different wavelengths. The results reveal that the RI of the mixture is simply a linear combination of the constituent RIs. Figure 9 shows the RI of 828/1510 resin mixtures (no curing agent) with similar results. These results show that specifying the RI of a cured or uncured epoxy resin is a simple task.
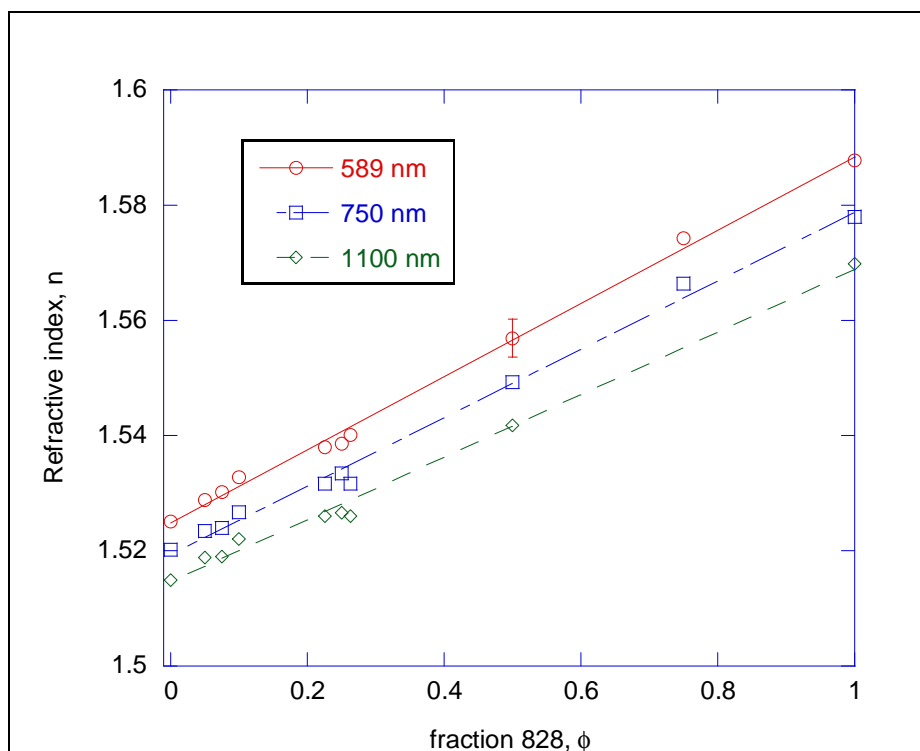
Figure 8. RI of Epon 828/Eponex 1510 epoxy resin mixtures cured with TETA.
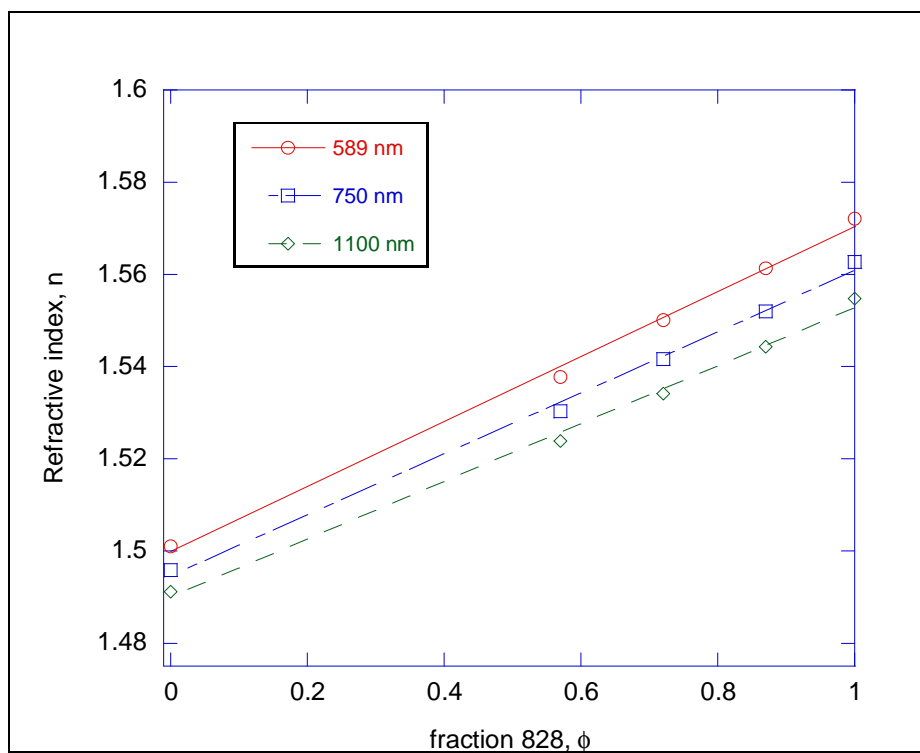

Figure 9. RI of Epon 828/Eponex 1510 mixture (resin only).

Figure 10 shows the RI of a 1510/828 epoxy over a range of NLO chromophore concentrations. As the figure shows, the presence of the dye increases the RI of the matrix significantly. From these data, we will assume that 10% dye will increase the matrix RI by ~0.015. Therefore, the ratio of 828 and 1510 should be adjusted accordingly, based on these results, to keep the matrix and reinforcement RI matched at this dye concentration.
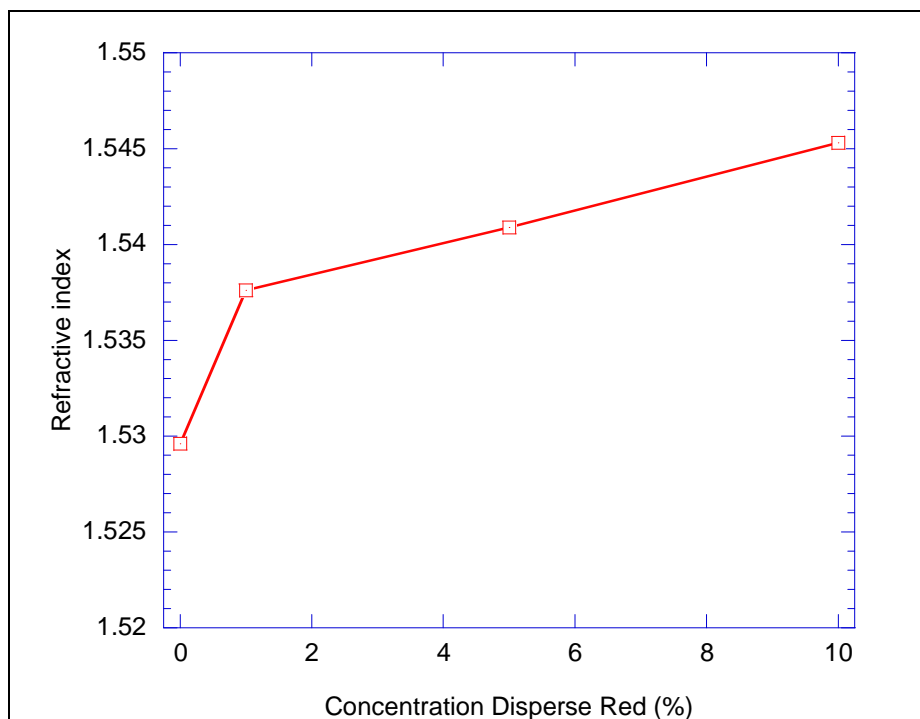

Figure 10. RI at 750 nm of TETA-cured 828/1510 (25/75%) mixture over a range of disperse red concentrations.

4.2   Deposition of Transparent Electrodes

Figure 11 shows ITO coatings deposited on glass slides at various ion energies. The results show that simply evaporated ITO is neither transparent nor conductive, whereas very low-energy ion bombardment results in electrically conductive films with optical transmissivity as high as 92%. The optimal ion energy observed is in the range 100–200 eV, while higher energy ion bombardment introduces more defects that reduce transparency. Rutherford backscattering spectrometry (RBS) (figure 12) shows that the oxygen ion beam produces stoichiometric ITO, while films deposited without oxygen ion beam assistance are oxygen-poor. Qualitative adhesion experiments using Scotch Tape[*] to attempt to remove the coatings showed that adhesion to glass, Mylar, and PMMA is high.

_____

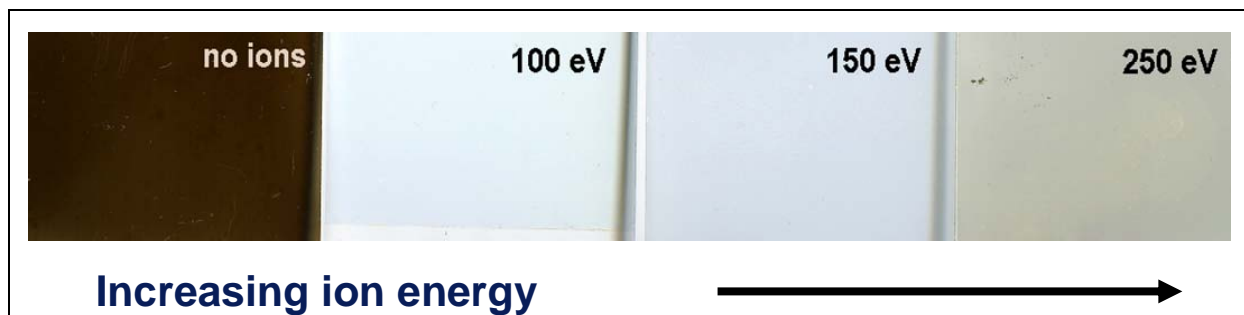[*]Scotch Tape is a registered trademark of 3M Corporation.

14

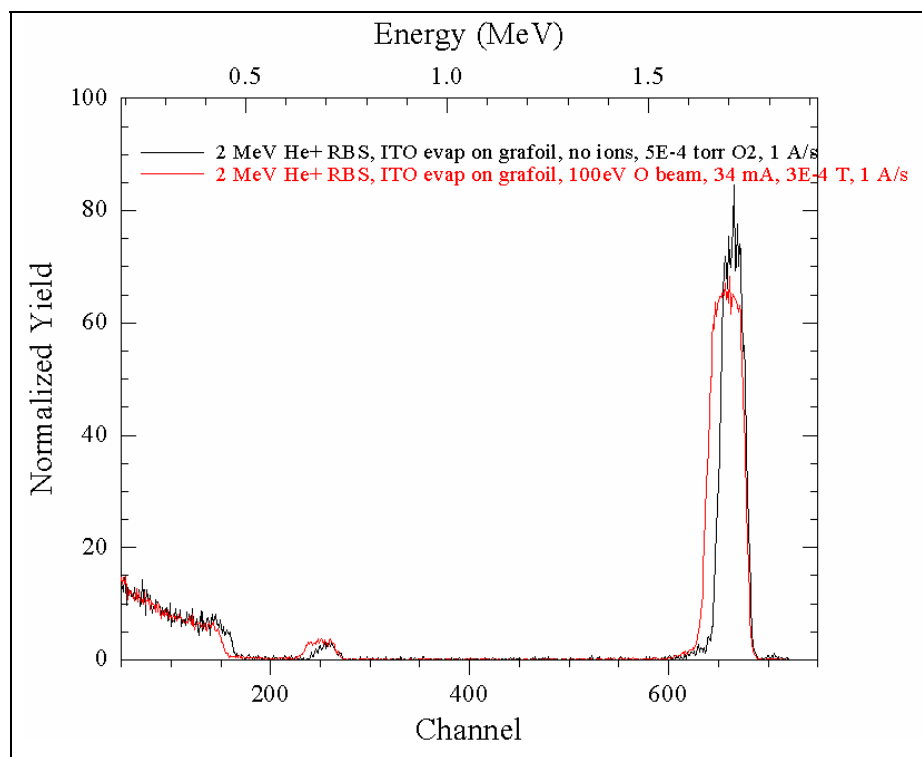Figure 11. ITO-coated glass slides produced with various ion energies.

Figure 12. RBS spectra of ITO films.

4.3   UV-Vis Experiments

Figure 13 shows results of 12 UV-Vis transmission experiments for the unpoled dye/epoxy/glass sample. The 12 experiments were performed in succession, switching from 0- to 1-kV potential electric fields across the specimen every two experiments. The plot shows that the electric field does not affect optical transmission through the specimen. Figure 14 shows data for similar experiments performed on the poled dye/epoxy/glass sample. For this specimen, there is a slight increase in transmission under an electric field; however, the change is very small (~0.1%).
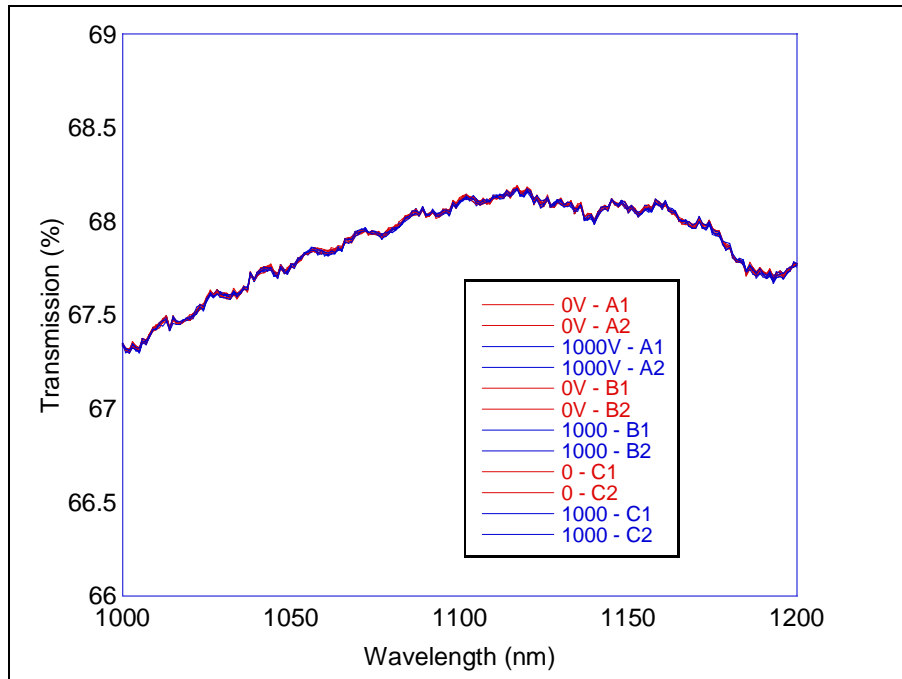
Figure 13. Transmission of unpoled dye/epoxy/glass samples over a range of wavelengths.
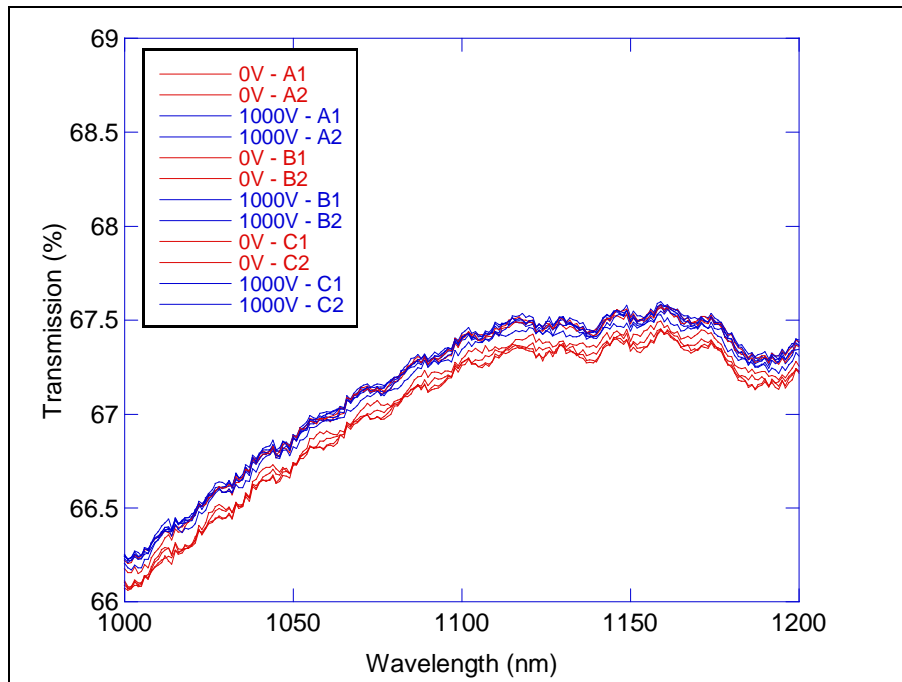

Figure 14. Transmission of poled dye/epoxy/glass samples over a range of wavelengths.

Figure 15 shows the results for transmission experiments at a single wavelength (1200 nm) of two samples. As before, the specimens were tested in succession switching from 0- and 1-kV potential electric fields across the specimen every two experiments. The points in the graph represent the averages of each experiment pair. As before, the specimen with the dye shows a small change in transmission, and the undyed specimen shows relatively no change with applied potential.

Figure 15. Relative change in transmission at 1200 nm of cured epoxy resins (with and without dye) under varying electric fields.

Figure 16 shows a similar experiment comparing the transmission through uncured resin composites, dyed and undyed. Since the change in transmission for these experiments is higher, the results seem to suggest that the uncured resin (matrix) does allow for more chromophore mobility. However, the undyed specimen shows a change in transmission that is similar in magnitude to the undyed specimen. This behavior is likely due to the birefringent nature of the epoxy resins themselves and the polarity of the resin molecules which align with electric field and induce a change in the RI through the thickness of the specimen.
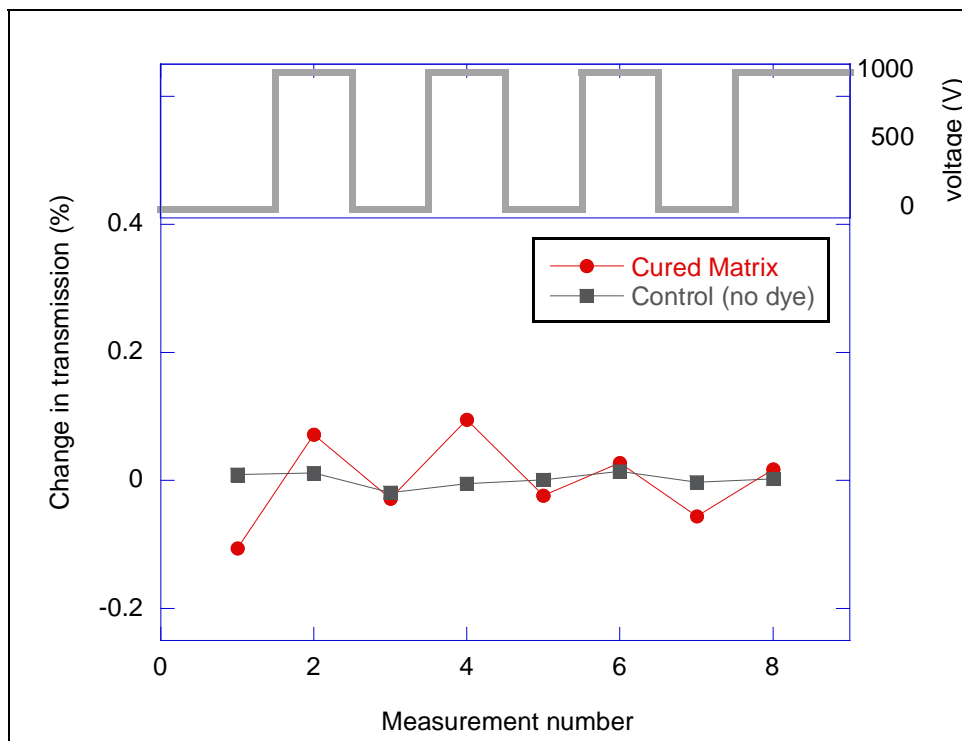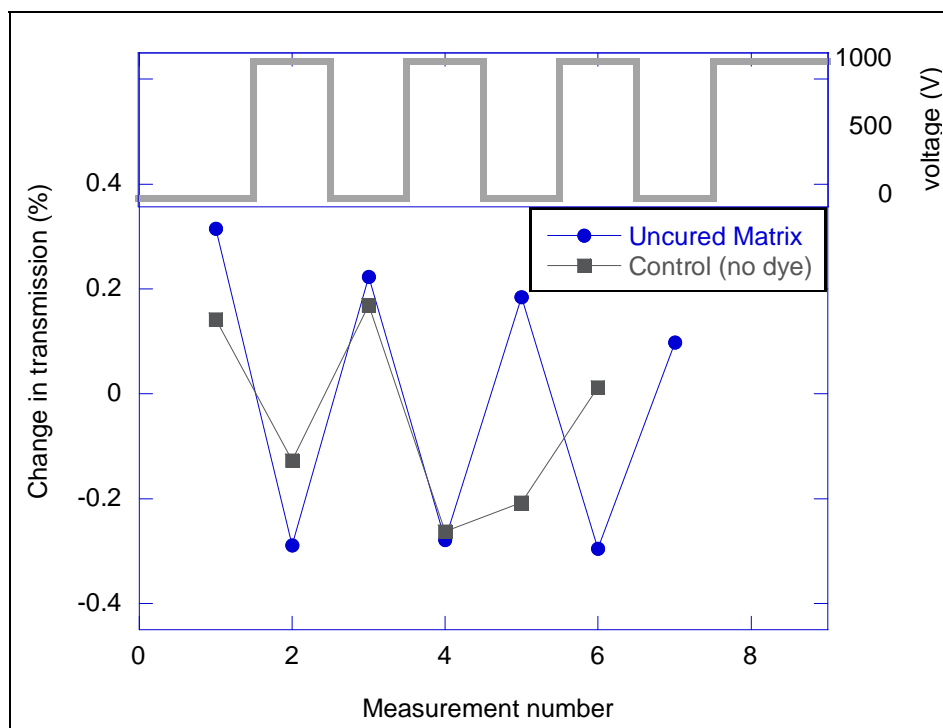
Figure 16. Relative change in transmission at 1200 nm of uncured epoxy resins (with and without dye) under varying electric fields.

4.4   Chromophore Synthesis

With respect to our approach to synthesize a highly conjugated NLO chromophore (figure 5), several attempts were made to generate the enol form and then trap it as either the methyl or silyl ether. Unfortunately, excessive side products were obtained from all attempts, so an alternative route may need to be investigated. However, a recent report in the literature (*8*) has validated the soundness of this approach, indicating the preparation of conjugated NLO materials using click chemistry. The difference between the published approach and this approach was the use of phenyl azides instead of α-keto azides. The phenyl azides generate a rigid conjugated system upon the cycloaddition, but they must have large solubilizing groups to prevent crystallization of the materials upon reaction. The compounds reported in the literature were also limited to symmetric molecules lacking the desired push-pull electron systems to enhance polarizability. Therefore, with additional investigation and molecule design, click chemistry may be amenable to the efficient preparation of polarizable NLO materials.

5.   Conclusions

In this report, we have studied an approach for rendering the matrix of a glass-polymer composite electro-optically active. Such active control over the matrix RI would make RI-matched polymer composites much more viable by allowing for correction of temperature-

induced RI changes in the matrix. We have found that the incorporation of a NLO chromophores into the matrix results in some modest control over the optical transmission through the matrix with applied electric field, perhaps due to a small change in the matrix RI. However, the change in transmission was very small, (~0.1%), and further study is needed to confirm the electro-optical behavior. Also, for the technology to be useful, it is necessary to increase the dynamic range significantly. Furthermore, the composite is not visibly transparent at the dye concentrations used in this project. While such a material would still be suitable as an impact resistant window, it was not possible to preserve visible transparency by minimizing chromophore content. A more attractive alternative is the use of a chromophore that does not absorb at visible wavelengths. Such a material has been reported by Herlocker et al. (*9*) and Kimura et al. (*10*). In addition to achieving visible transparency, it is also necessary to synthesize and incorporate better chromophores with higher electro-optical coefficients, which results in greater control over RI. To that end, we have begun studying easy synthesis routes to new higher-response chromophore molecules via click chemistry.

It is also necessary to develop experimental capability for measuring individual components of the RI tensor at infrared wavelengths in order to measure the RI as a function of electric field. In this work, we attempted to infer an electric field-dependent change in RI from the change in transmitted intensity through the induced RI mismatch between NLO matrix and E-glass reinforcement. Developing the capability to measure the change in matrix RI directly would lead to better understanding and design of the electro-optical composites.

6. References

1. Iba, H.; Kagawa, Y. Light Transmittance of Continuous Fibre-Reinforced Composites: Analysis, Model Experiment and Parametric Study. *Philosophical Magazine B* **1998**, *78* (1), 37–52.

2. Weaver, K. D.; Stoffer, J. O.; Day, D. E. Preparation and Properties of Optically Transparent, Pressure-Cured Poly(Methacrylate) Composites. *Polymer Composites* **1993**, *14* (6), 515–523.

3. Kippelen, B.; Peyghambarian, N. Photorefractive Polymers and their Applications. *Advances in Polymer Science* **2003**, *161*, 87–156.

4. Ambrosanio, P.; Centore, R.; Concilio, S.; Panunzi, B.; Sirigu, A.; Tirelli, N. Synthesis and Characterization of Polyesters With Nonlinear Optical Properties. *Polymer* **1999**, *40*, 4923–4928.

5. Thackara, J.; Jurich, M.; Swalen, J. Electro-Optic Measurements of Tolane-Based Polymeric Phase Modulators. *Journal of the Optical Society of America B* **1994**, *11* (5), 835–839.

6. Mao, S.; Ra, Y.; Guo, L.; Zhang, C.; Dalton, L. Progress Towards Device-Quality Second-Order Nonlinear Optical Materials. 1. Influence of Processing Conditions On Nonlinearity, Temporal Stability, and Optical Loss. *Chemistry of Materials* **1998**, *10*, 146–155.

7. Kolb, H. C.; Finn, M. G.; Sharpless, K. B. Click Chemistry: Diverse Chemical Function From a Few Good Reactions. *Angewandte Chemie* **2001**, *40* (11), 2004–2021.

8. Parent, M.; Mongin, O.; Kamada, K.; Katan, C.; Blanchard-Desce, M. *Chem. Comm.* **2005**, 2029–2031.

9. Herlocker, J. A.; Ferrio, K. B.; Hendrickx, E.; Guenther, B. D.; Mery, S.; Kippelen, B.; Peyghambarian, N. Direct Observation of Orientation Limit in a Fast Photorefractive Polymer Composite. *Applied Physics Letters* **1999**, *74* (16), 2253–2255.

10. Kimura, T.; Fukuda, T.; Matsuda, H.; Kato, M.; Nakanishi, H. Development of Second-Order Nonlinear Optical Polymers Without Visible Absorption. *Kobunshi Ronbunshu* **2003**, *60* (12), 682–692.

    1   DEFENSE TECHNICAL
  (PDF   INFORMATION CTR
 ONLY)   DTIC OCA
           8725 JOHN J KINGMAN RD
           STE 0944
           FORT BELVOIR VA 22060-6218

    1   US ARMY RSRCH DEV &
           ENGRG CMD
           SYSTEMS OF SYSTEMS
           INTEGRATION
           AMSRD SS T
           6000 6TH ST STE 100
           FORT BELVOIR VA 22060-5608

    1   DIRECTOR
           US ARMY RESEARCH LAB
           IMNE ALC IMS
           2800 POWDER MILL RD
           ADELPHI MD 20783-1197

    3   DIRECTOR
           US ARMY RESEARCH LAB
           AMSRD ARL CI OK TL
           2800 POWDER MILL RD
           ADELPHI MD 20783-1197

       ABERDEEN PROVING GROUND

    1   DIR USARL
           AMSRD ARL CI OK TP (BLDG 4600)

ABERDEEN PROVING GROUND

```
9      DIR USARL
       AMSRD ARL WM MA
         M VAN LANDINGHAM
         D O BRIEN (3 CPS)
         J ORLICKI
         J DEMAREE
         J HIRVONEN
       AMSRD ARL WM MD
         J PATEL
         J SANDS
```